

# Red-Emitting Thermally Activated Delayed Fluorescence Polymers with Poly(fluorene-co-3,3'-dimethyl diphenyl ether) as the Backbone

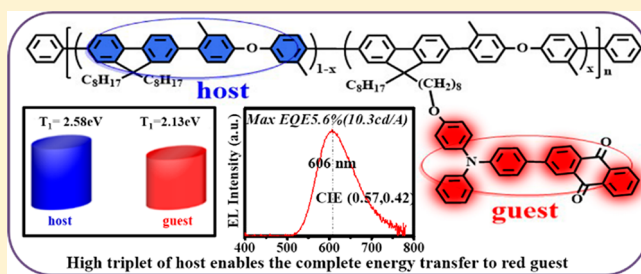
Yun Yang,<sup>†,‡</sup> Lei Zhao,<sup>†</sup> Shumeng Wang,<sup>\*,†</sup> Junqiao Ding,<sup>\*,†,‡</sup> and Lixiang Wang<sup>†,‡</sup>

<sup>†</sup>State Key Laboratory of Polymer Physics and Chemistry, Changchun Institute of Applied Chemistry, Chinese Academy of Sciences, Changchun 130022, P. R. China

<sup>‡</sup>University of Science and Technology of China, Hefei 230026, P. R. China

## Supporting Information

**ABSTRACT:** A series of red-emitting thermally activated delayed fluorescence (TADF) polymers have been designed and synthesized based on poly(fluorene-co-3,3'-dimethyl diphenyl ether) (PFDMPPE) as the backbone. Compared with polyfluorene (PF, 2.16 eV), the introduction of 3,3'-dimethyl diphenyl ether into the main chain of PFDMPPE leads to the increased triplet energy of 2.58 eV, which is higher enough than the tethered red TADF guest (2.13 eV) to prevent the unwanted triplet energy back-transfer. Meanwhile, there is a good overlap between the absorption spectrum of the red guest and the photoluminescence (PL) spectrum of the polymeric host, ensuring the efficient energy transfer from host to guest. Consequently, the resultant polymers PFDMPPE-R01 to PFDMPPE-R10 in solid states show obvious red TADF properties with delayed fluorescence lifetimes of 126–191  $\mu$ s and PL quantum yields of 0.18–0.55. Among them, PFDMPPE-R05 obtains the best device performance, revealing a bright red electroluminescence peaked at 606 nm and a promising current efficiency of 10.3 cd/A (EQE = 5.6%). The results compete well with those of red phosphorescent polymers and indicate that PFDMPPE other than PF is a suitable polymeric host for the construction of efficient red TADF polymers.



High triplet of host enables the complete energy transfer to red guest

## 1. INTRODUCTION

Since Friend et al. demonstrated the electroluminescence (EL) from poly(*p*-phenylenevinylene) (PPV) in 1990,<sup>1</sup> numerous conjugated and nonconjugated polymers based on fluorescence, phosphorescence, and thermally activated delayed fluorescence (TADF) have been explored for high-performance polymer light-emitting diodes (PLEDs).<sup>2–7</sup> Among them, fluorescent polymers suffer from the limited internal quantum efficiency (IQE) below 25% because 75% of the electrically generated triplet excitons are dissipated as heat.<sup>2,8,9</sup> The bottleneck is broken by phosphorescent polymers, which can harvest both singlet and triplet excitons to realize a theoretical 100% IQE.<sup>3,10</sup> However, these phosphorescent polymers seem to be rather expensive and unsustainable given that they contain Ir(III), Pt(II), and Os(II) complexes and so forth. Therefore, an alternative approach for 100% IQE is developed using TADF polymers without any rare metals.<sup>6,7,11</sup> Thanks to their small energy difference ( $\Delta E_{ST}$ ) between the lowest singlet ( $S_1$ ) and triplet excited states ( $T_1$ ), triplet excitons can be upconverted from  $T_1$  to  $S_1$  by absorbing environmental thermal energy and then radiatively decay from  $S_1$  to yield delayed fluorescence.<sup>12</sup>

In view of the anticipated high efficiency and low cost, nowadays much attention has been paid for the development of TADF polymers showing different emissive colors.<sup>13–19</sup> For

example, Cheng et al. designed a series of conjugated polymers with a backbone-donor/pendant-acceptor architecture, revealing bright orange TADF accompanied by an external quantum efficiency (EQE) up to 19.4% and Commission Internationale de L'Eclairage (CIE) coordinates of (0.51, 0.47).<sup>14</sup> With an insulating backbone and varying ratios of 2-(10*H*-phenothiazin-10-yl)dibenzothiophene-*S,S*-dioxide as a pendant TADF unit, Bryce et al. reported green-emitting TADF polymers and obtained a maximum EQE of 20.1% and CIE coordinates of (0.36, 0.55).<sup>15</sup> Until recently, a novel molecular design for blue-emitting TADF polymers has been proposed based on a nonconjugated polyethylene backbone with through-space charge transfer effect between pendant electron donor (D) and acceptor (A) units. A high EQE of 12.1% was achieved together with CIE coordinates of (0.18, 0.27).<sup>17</sup> It should be noted that the EL wavelength of most reported TADF polymers mainly covers 470–590 nm, and there are few studies on red-emitting ones with an emission peak above 600 nm.<sup>20</sup>

Here we report the design and synthesis of red-emitting TADF polymers for efficient PLEDs. As depicted in Figure 1, a

**Received:** September 24, 2018

**Revised:** November 14, 2018

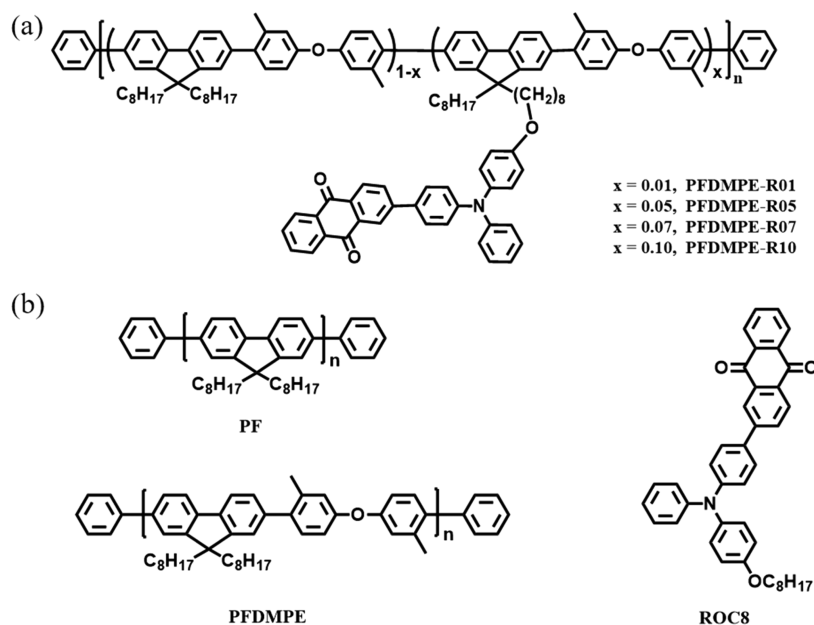


Figure 1. Molecular structures of red-emitting TADF polymers (a) and the corresponding polymeric hosts and red dopant (b).

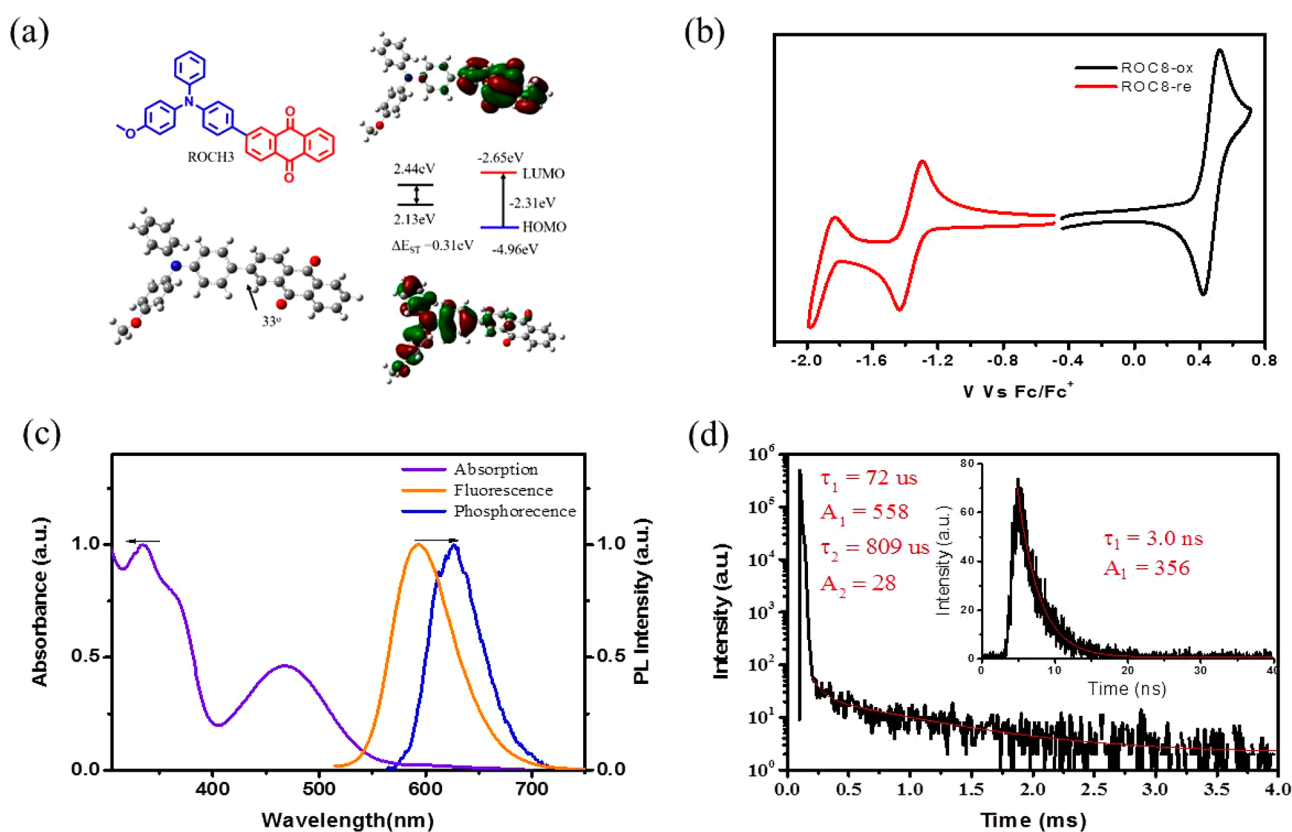
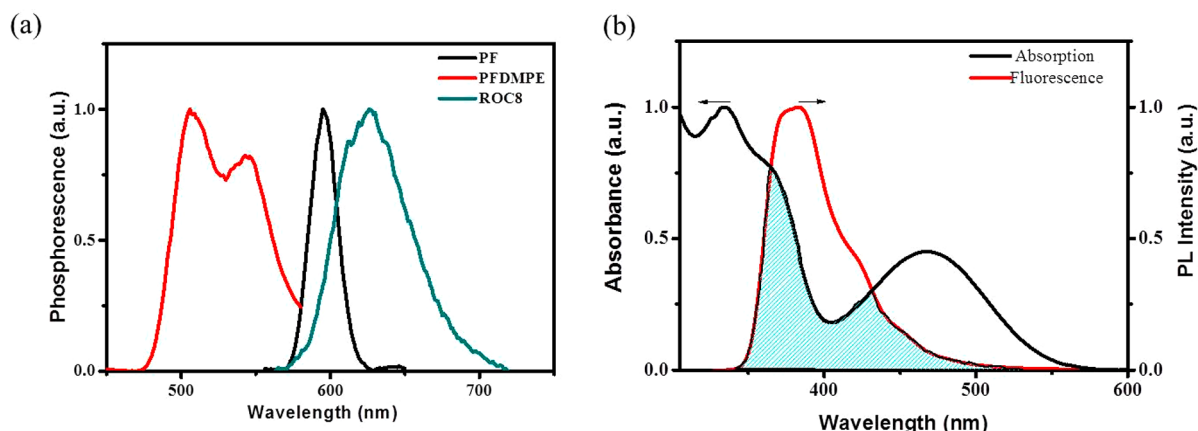


Figure 2. Photophysical and electrochemical properties of ROC8. (a) Chemical structure as well as HOMO and LUMO distributions simulated by TD-DFT at the B3LYP/6-31G\* level. For simplicity, octyloxy is replaced with methoxy. (b) CV curves in DCM and THF for anodic and cathodic sweeping, respectively. (c) UV-vis absorption, fluorescence, and phosphorescence spectra in toluene. (d) Transient decay spectra in an  $O_2$ -free cyclohexane.

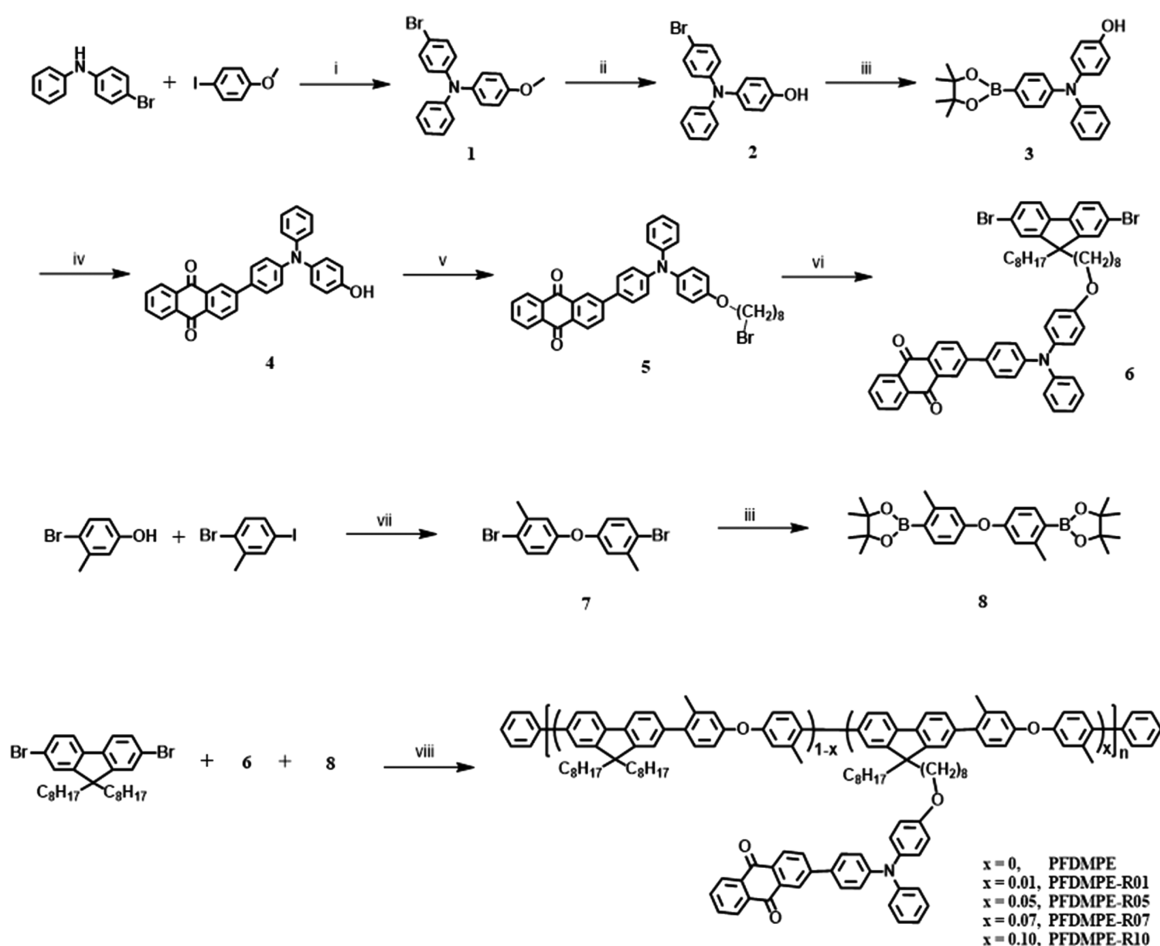
red TADF emitter 2-(*N*-(4-octyloxyphenyl)diphenylamino)-4'-anthraquinone (ROC8) acts as the side chain. At the same time, poly(fluorene-*co*-3,3'-dimethyl diphenyl ether) (PFDMPPE) with a triplet energy higher than polyfluorene (PF) is used as the backbone to avoid the unwanted loss of

triplet excitons. Consequently, the resultant polymers PFDMPPE-R01 to PFDMPPE-R10 can well maintain the TADF property of ROC8 benefiting from the effective energy transfer from PFDMPPE to ROC8 in solid states. Among them, PFDMPPE-R05 displays the best device performance and gives



**Figure 3.** (a) Phosphorescence spectra of PF and PFDMPPE in film compared with that of ROC8 in toluene under 77 K. (b) PL spectrum of PFDMPPE in film and UV-vis absorption spectrum of ROC8 in toluene. The shadow part shows their overlap.

### Scheme 1. Synthetic Route of Red-Emitting TADF Polymers<sup>a</sup>



<sup>a</sup>Reagents and conditions: (i) 1,10-phenanthroline monohydrate, CuI, toluene, 110 °C; (ii) BBr<sub>3</sub>, DCM, 0 °C to rt; (iii) bis(pinacolato)diboron, Pd(dppf)Cl<sub>2</sub>, KOAc; (iv) 2-bromoanthracene-9,10-dione, Pd(PPh<sub>3</sub>)<sub>4</sub>, K<sub>2</sub>CO<sub>3</sub>, Aliquat 336, H<sub>2</sub>O, toluene, 110 °C; (v) 1,8-dibromooctane, tetrabutylammonium bromide, K<sub>2</sub>CO<sub>3</sub>, THF, 75 °C; (vi) 2,7-dibromo-9-octyl-9H-fluorene, KOH, DMF, 70 °C; (vii) 2,2,6,6-tetramethylheptane-3,5-dione, CuI, Cs<sub>2</sub>CO<sub>3</sub>, DMF, 110 °C; (viii) Pd<sub>2</sub>(Dba)<sub>3</sub>, S-Phos, Aliquat 336, K<sub>2</sub>CO<sub>3</sub>, H<sub>2</sub>O, toluene, 96 °C.

a bright red EL peaked at 606 nm with a promising EQE of 5.6% and current efficiency of 10.3 cd/A.

## 2. RESULTS AND DISCUSSION

**2.1. Molecular Design.** According to the literature,<sup>21</sup> anthraquinone-based D–A–D type TADF materials have been

reported to emit an efficient red light with a peak wavelength of 624 nm and EQE of 12.5%. Promoted by this result, a simple D–A type TADF emitter ROC8 is then designed based on anthraquinone as A and triphenylamine as D (Figure 1). Meanwhile, an alkoxy group is introduced into triphenylamine to favor the next linkage between the TADF guest and

polymeric host. The ground state geometry of ROC8 is optimized using TD-DFT at the B3LYP/6-31G\* level in the gas phase (Figure 2a). The highest occupied molecular orbital (HOMO) is mainly distributed on the alkoxy-functionalized triphenylamine, whereas the lowest unoccupied molecular orbital (LUMO) is localized on anthraquinone. The observed good HOMO and LUMO separation leads to a relatively low  $\Delta E_{ST}$  (0.31 eV for calculated value; 0.18 eV for experimental value), which is beneficial for the effective upconversion from  $T_1$  to  $S_1$ . Because of the small twisted dihedral angle between anthraquinone and alkoxy-functionalized triphenylamine (33 °C), moreover, there exists a partial molecular orbital overlap on the linked phenyl ring of anthraquinone to ensure a certain oscillator strength and high photoluminescence quantum yield (PLQY).<sup>22</sup> Cyclic voltammetry (CV) was then used to investigate the electrochemical property of ROC8 (Figure 2b). Both reversible oxidation and reduction processes appear during the anodic and cathodic sweepings, and the HOMO and LUMO energy levels of ROC8 are determined to be  $-5.21$  and  $-3.51$  eV, respectively. In addition, ROC8 exhibits a distinct absorption band in the range 400–550 nm (Figure 2c), which can be ascribed to the charge transfer (CT) state from alkoxy-functionalized triphenylamine to anthraquinone. A maximum emission at about 593 nm is also observed for the PL spectrum of ROC8 in cyclohexane together with a moderate PLQY of 0.24. The corresponding prompt and delayed fluorescent lifetimes are found to be 3.0 ns and 338  $\mu$ s, respectively (Figure 2d). The values match well with the D–A–D type red TADF emitters<sup>21</sup> and clearly indicate the TADF nature of ROC8.

On the other hand, as for side-chain type TADF polymers, the triplet energy of the polymeric host is required to be larger than that of the tethered TADF guest so as to prevent the triplet energy back-transfer (TEBT) from guest to host.<sup>6,23–25</sup> Unfortunately, PF has a triplet energy of about 2.16 eV (Figure 3a), very close to that of ROC8 (2.13 eV). So 3,3'-dimethyl diphenyl ether is incorporated into PF to interrupt the conjugation length of the backbone. And the resultant polymeric host PFDMPPE shows an enhanced triplet energy of 2.58 eV, high enough to avoid the TEBT from ROC8 to PFDMPPE. Furthermore, there is a good overlap between the absorption spectrum of ROC8 and the PL spectrum of PFDMPPE (Figure 3b). The observation implies the efficient energy transfer from PFDMPPE to ROC8, which will be discussed below. With these considerations, it is expected that PFDMPPE other than PF can act as the good host of ROC8 for the construction of red-emitting TADF polymers.

**2.2. Synthesis and Characterization.** The synthetic route of polymers PFDMPPE-R01 to PFDMPPE-R10 is shown in Scheme 1. Starting from the commercially available 4-bromo-*N*-phenylaniline and 1-iodo-4-methoxybenzene, 4-bromo-*N*-(4-methoxyphenyl)diphenylamine (**1**) was prepared via a C–N coupling, followed by demethylation and boric acid esterification to give 4-(4,4,5,5-tetramethyl-1,3,2-dioxaborolan-2-yl)-*N*-(4-hydroxyphenyl)diphenylamine (**3**). Then a Suzuki–Miyaura coupling was performed between **3** and 2-bromoanthraquinone to produce 2-(*N*-(4-hydroxyphenyl)diphenylamino)-4'-anthraquinone (**4**), which was attached to 2,7-dibromo-9-octyl-9*H*-fluorene through a nonconjugated linkage to form the key monomer 2-(*N*-(4-((8-(2,7-dibromo-9-octylfluoren-9-yl)octyl)oxy)phenyl)diphenylamino)-4'-anthraquinone (**6**). At the same time, after a selective Ullmann reaction between 4-bromo-3-methylphenol and 1-bromo-4-

iodo-2-methylbenzene, 4,4'-oxybis(1-bromo-2-methylbenzene) (**7**) was obtained and converted to its corresponding borate 2,2'-(oxybis(2-methyl-4,1-phenylene))bis(4,4,5,5-tetramethyl-1,3,2-dioxaborolane) (**8**). Finally, with 7-dibromo-9,9-dioctyl-9*H*-fluorene, **6** and **8** in hand, a typical Suzuki polymerization using  $\text{Pd}_2(\text{dba})_3$  as the catalyst and S-Phos as the ligand was adopted to synthesize the red-emitting TADF polymers PFDMPPE-R01 to PFDMPPE-R10. As determined by gel permeation chromatography (GPC), the number-average molecular weights ( $M_n$ ) and polydispersity index (PDI) of PFDMPPE-R01 to PFDMPPE-R10 are about 83–149 kDa and 1.6–1.8, respectively (Table 1), and they are found to be

**Table 1. Physical Properties of Red-Emitting TADF Polymers PFDMPPE-R01 to PFDMPPE-R10 Compared with the PFDMPPE Backbone**

polymers	ROC8 in the polymers (mol %)		$M_n^b$ (kDa)	PDI <sup>b</sup>	$T_g^c$ (°C)	$T_d^d$ (°C)
	feed ratio	actual ratio <sup>a</sup>				
PFDMPPE	0	0	149	1.6	86	403
PFDMPPE-R01	0.010	0.010	120	1.6	88	424
PFDMPPE-R05	0.050	0.048	132	1.7	88	427
PFDMPPE-R07	0.070	0.064	126	1.7	86	429
PFDMPPE-R10	0.100	0.096	83	1.8	87	428

<sup>a</sup>Calculated from the <sup>1</sup>H NMR spectra. <sup>b</sup>Determined by GPC in THF using polystyrene as the standard. <sup>c</sup>Glass transition temperatures determined by TGA in N<sub>2</sub>. <sup>d</sup>Decomposition temperatures corresponding to a 5% weight loss.

thermally stable with decomposition temperatures over 400 °C and glass transition temperatures close to 90 °C (Figure S1). Noticeably, the introduced content of ROC8 into the polymer can be calculated quantitatively from their <sup>1</sup>H NMR. There are two characteristic proton signals at 8.34 and 8.51 ppm originating from ROC8, which could be distinguished from those of PFDMPPE (Figure 4). Hence, by comparison of the integrals of these two signals related to all the signals, the actual ROC8 content is estimated to be well comparable to the feed ratio. This suggests that the red TADF fragment ROC8 has been successfully incorporated into the backbone of PFDMPPE during polymerization.

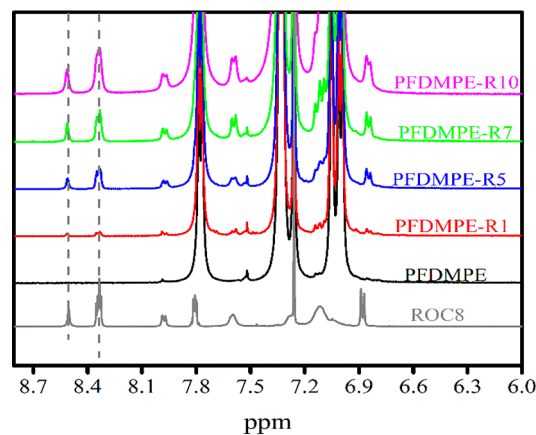


**Figure 4.** <sup>1</sup>H NMR spectra of red-emitting TADF polymers PFDMPPE-R01 to PFDMPPE-R10 compared with PFDMPPE and ROC8.

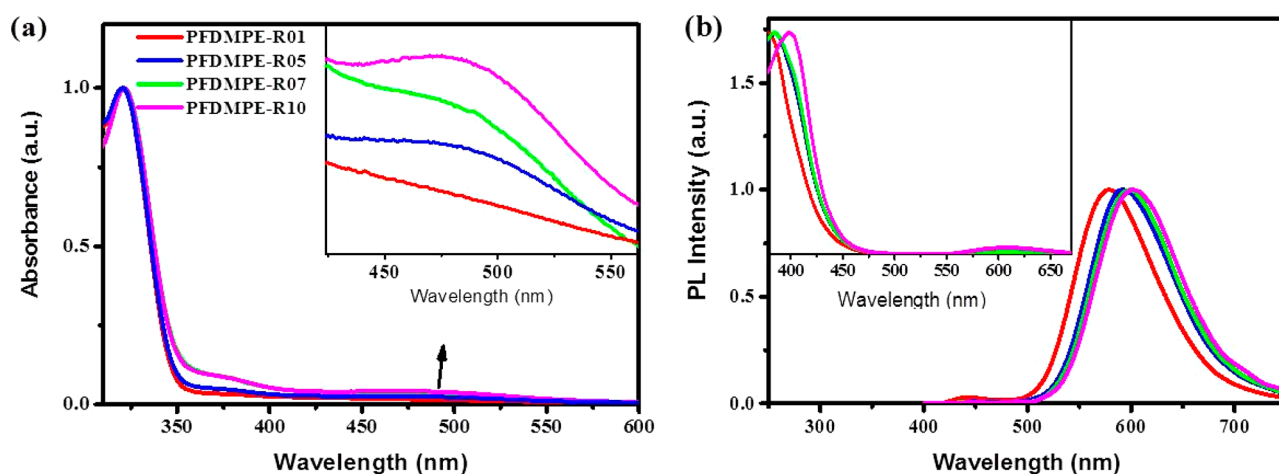


**Figure 5.** (a) UV-vis absorption spectra in films for red-emitting TADF polymers PFDMPPE-R01 to PFDMPPE-R10 (inset: CT absorption). (b) Their corresponding PL spectra in films (inset: PL spectra in toluene).

**Table 2. Photophysical Properties of Red-Emitting TADF Polymers PFDMPPE-R01 to PFDMPPE-R10 Compared with ROC8**

compounds	$\lambda_{\text{abs}}^a$ [nm]	$\lambda_{\text{em}}^a$ [nm]	$\Phi_{\text{em}}^b$	$\tau_p^c$ [ns]	$\tau_d^c$ [us]	$S_1/T_1/\Delta E_{\text{ST}}^d$ [eV]
ROC8	334/365/469	593	0.24	3.0	338	2.31/2.13/0.18
PFDMPPE-R01	320/379/492	579	0.55	9.6	191	
PFDMPPE-R05	320/378/491	592	0.32	4.2	126	
PFDMPPE-R07	320/376/494	598	0.27	4.5	132	
PFDMPPE-R10	321/378/500	602	0.18	4.5	145	

<sup>a</sup>Measured in toluene for ROC8 and in film for red-emitting TADF polymers. <sup>b</sup>Measured by integrating sphere in degassed toluene for ROC8 and in film under  $N_2$  for red-emitting TADF polymers. <sup>c</sup>Measured in degassed cyclohexane for ROC8 and in film under  $N_2$  for red-emitting TADF polymers, and the prompt and delayed lifetimes ( $\tau_p$  and  $\tau_d$ ) were calculated using  $\tau_{\text{av}} = \sum A_i \tau_i^2 / \sum A_i \tau_i$ . <sup>d</sup> $S_1$  and  $T_1$  were estimated from the onset of the fluorescence and phosphorescence spectra, and  $\Delta E_{\text{ST}}$  is the difference between  $S_1$  and  $T_1$ .

**2.3. Photophysical Properties.** Figure 5 illustrates the UV-vis and PL spectra for PFDMPPE-R01 to PFDMPPE-R10 in films. As can be clearly seen, all the polymers exhibit one intense absorption band peaked at 320 nm together with two weak but discernible absorption bands in the ranges 350–400 and 400–550 nm (Figure 5a). According to the UV-vis spectrum of ROC8, the former could be reasonably attributed to the absorption of the polymeric backbone PFDMPPE, and the latter two are from the attached red TADF emitter ROC8. Additionally, except for PFDMPPE-R01 with an emission residue of PFDMPPE, an almost complete energy transfer from PFDMPPE to ROC8 is observed, leading to only ROC8 emission for PFDMPPE-R05, PFDMPPE-R07, and PFDMPPE-R10 (Figure 5b). By contrast, the emission from PFDMPPE dominates their whole PL spectra in solution associated with a very weak emission from ROC8 (inset in Figure 5b). The difference indicates that the intermolecular other than intramolecular energy transfer plays an important role on the photophysical properties of PFDMPPE-R01 to PFDMPPE-R10 in solid states.<sup>26</sup> With the increasing feed ratio, moreover, the emission maxima are obviously red-shifted from 579 nm of PFDMPPE-R01 to 602 nm of PFDMPPE-R10 because of the existing aggregation. Correspondingly, the measured PLQY is reduced from 0.55 of PFDMPPE-R01 to 0.18 of PFDMPPE-R10 (Table 2).<sup>27</sup>

To probe the TADF properties of these polymers, their transient PL spectra in neat films were also recorded under nitrogen at 298 K. A prompt fluorescent lifetime of 9.6 ns as well as a delayed fluorescent lifetime of 191  $\mu$ s is observed for PFDMPPE-R01 (Figure 6); PFDMPPE-R05, PFDMPPE-R07, and

PFDMPPE-R10 display delayed emissions with a similar lifetime of 126–145  $\mu$ s in addition to prompt emissions with a similar lifetime of 4.2–4.5 ns. As mentioned above, the complete energy transfer from the polymeric host to the attached TADF fragment may contribute to the shorter lifetimes of PFDMPPE-R05, PFDMPPE-R07, and PFDMPPE-R10 compared with PFDMPPE-R01.<sup>28,29</sup> Albeit this, they all emit delayed fluorescence to some degree as a result of an initial intersystem crossing (ISC) to the triplet state followed by repopulation of the singlet state via reverse intersystem crossing (RISC).<sup>30</sup> With PFDMPPE-R05 as an example, the temperature dependence of the transient PL is also investigated in the temperature range 80–300 K (Figure S2). As one can see, the delayed emission is gradually decreased when temperature is down from 300 to 150 K. This means that the efficient  $T_1$  to  $S_1$  upconversion activated by the thermal energy is weakened, which is a direct evidence of TADF, and the conversely enhanced delayed emission from 150 to 80 K can be tentatively ascribed to the predominant phosphorescence under low temperature, consistent with the literature.<sup>31</sup>

**2.4. EL Properties.** To evaluate the EL properties of PFDMPPE-R01 to PFDMPPE-R10, PLEDs were fabricated with a structure of ITO/PEDOT:PSS (50 nm)/EML (40 nm)/TmPyPB (50 nm)/LiF (1 nm)/Al. Here PEDOT:PSS stands for poly(3,4-ethylenedioxythiophene:poly(styrenesulfonate)) and serves as the hole-injection layer; TmPyPB stands for 1,3,5-tri(*m*-pyrid-3-ylphenyl)benzene and acts as the electron-transporting layer;<sup>32</sup> and the red-emitting TADF polymers PFDMPPE-R01 to PFDMPPE-R10 are used as the emitting layer (EML). Figure 7a–d plots the EL spectra, current density–

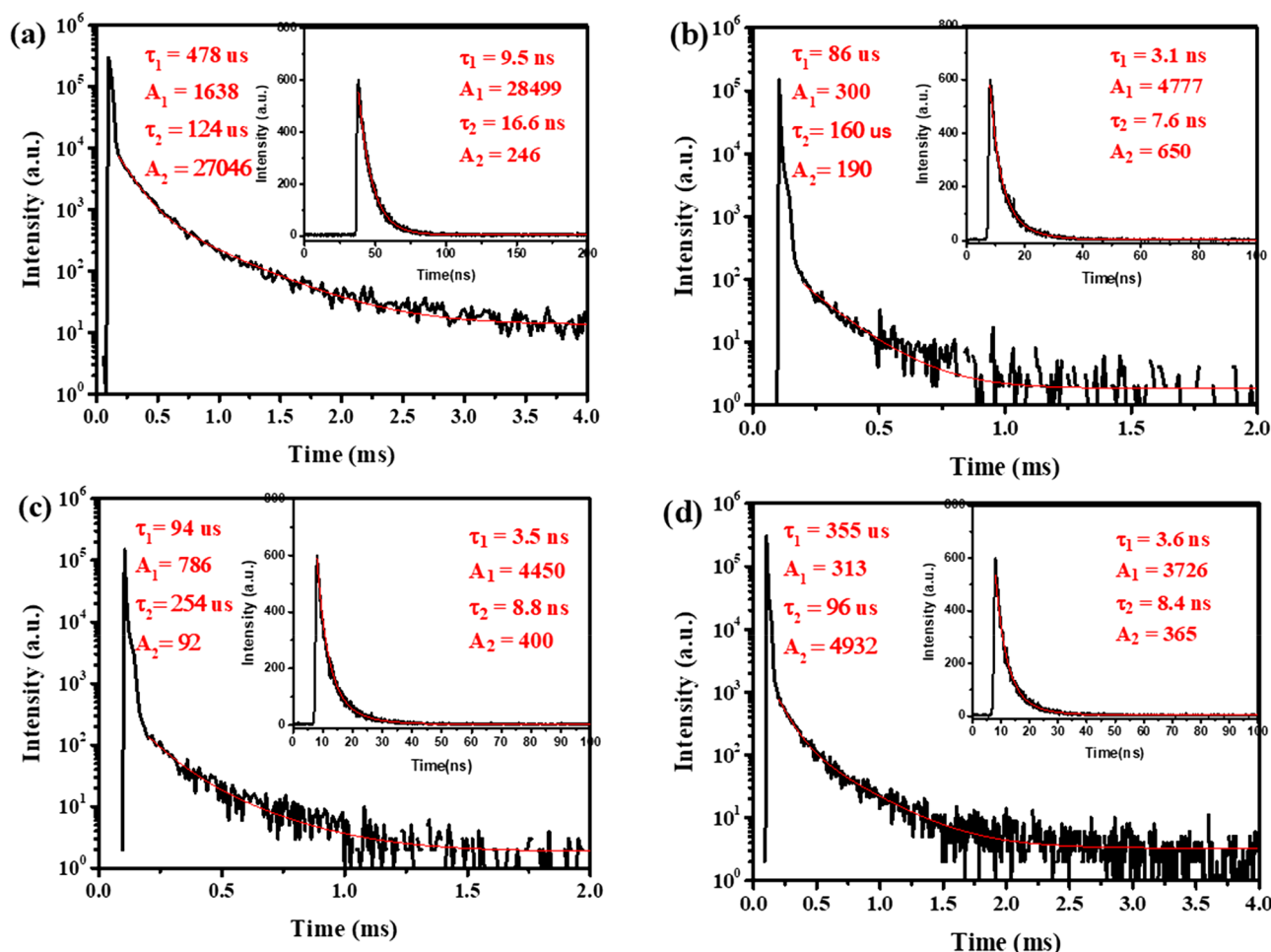


**Figure 6.** Transient decay spectra in films for PFDMPPE-R01 (a), PFDMPPE-R05 (b), PFDMPPE-R07 (c), and PFDMPPE-R10 (d).

voltage, and luminance–voltage characteristics together with the current density dependence of current efficiency and EQE. The device performance is also summarized in Table 3. As one can see, the EL is only from the red-emitting TADF polymers although a small bathochromic shift is observed with respect to their PL counterparts (Figure 7a). When the introduced ROC8 content in the polymer increases from PFDMPPE-R01 to PFDMPPE-R10, the EL spectra turn out to shift toward a long wavelength, and an improved energy transfer efficiency is obtained. Besides the major emission from the TADF guest, PFDMPPE-R01 still shows an obvious emission from the polymeric host, whereas this residue is completely quenched for PFDMPPE-R05, PFDMPPE-R07, and PFDMPPE-R10. Their EL maxima are 591, 606, 607, and 611 nm together with corresponding CIE coordinates of (0.49, 0.42), (0.57, 0.42), (0.58, 0.42), and (0.59, 0.41), respectively.

It should be noted that the current density at the same driving voltage first decreases from PFDMPPE-R01 to PFDMPPE-R05 and PFDMPPE-R07 and then goes up considerably to PFDMPPE-R10 (Figure 7b). Given that the HOMO/LUMO levels of ROC8 (−5.20/−3.51 eV) locate between those of PFDMPPE (−6.03/−2.44 eV), ROC8 may act as charge trap at a low doping concentration and lead to the observed reduced current density for PFDMPPE-R05 and PFDMPPE-R07. As the concentration of ROC8 elevates to about 10%, carriers are not first injected into PFDMPPE and then trapped by ROC8 but directly injected into ROC8. In this

case, the favored charge injection and enhanced current density are expected for PFDMPPE-R10. Therefore, among these polymers, PFDMPPE-R05 achieves the best device performance, revealing a maximum luminance of 1677 cd/m<sup>2</sup>, a peak current efficiency of 10.3 cd/A, and a peak EQE of 5.6% (Figure 7c,d). The results can compete well with red-emitting phosphorescent polymers,<sup>33–35</sup> indicating the great potential of red-emitting TADF polymers used for high-performance PLEDs. Also, we note that the EQE decays significantly to 1.05% at a high luminance of 500 cd/m<sup>2</sup> (Figure S3 and Table 3). Similar to the literature,<sup>21</sup> the long delayed lifetime above 100  $\mu$ s may be responsible for the observed severe efficiency roll-off induced by triplet–triplet annihilation.

### 3. CONCLUSIONS

In summary, we demonstrate a series of red-emitting TADF polymers with poly(fluorene-co-3,3'-dimethyl diphenyl ether) as the backbone. Owing to its higher triplet energy than the red guest and the good overlap between the guest absorption and the host PL, an effective energy transfer is anticipated for the resultant polymers PFDMPPE-R01 to PFDMPPE-R10 in solid states. As a result, they can well maintain the TADF property from the tethered guest, giving a peak current efficiency of 10.3 cd/A (EQE = 5.6%) and a bright red EL peaked at 606 nm. This work, we believe, will shed light on the development of red-emitting TADF polymers for high-performance PLEDs.

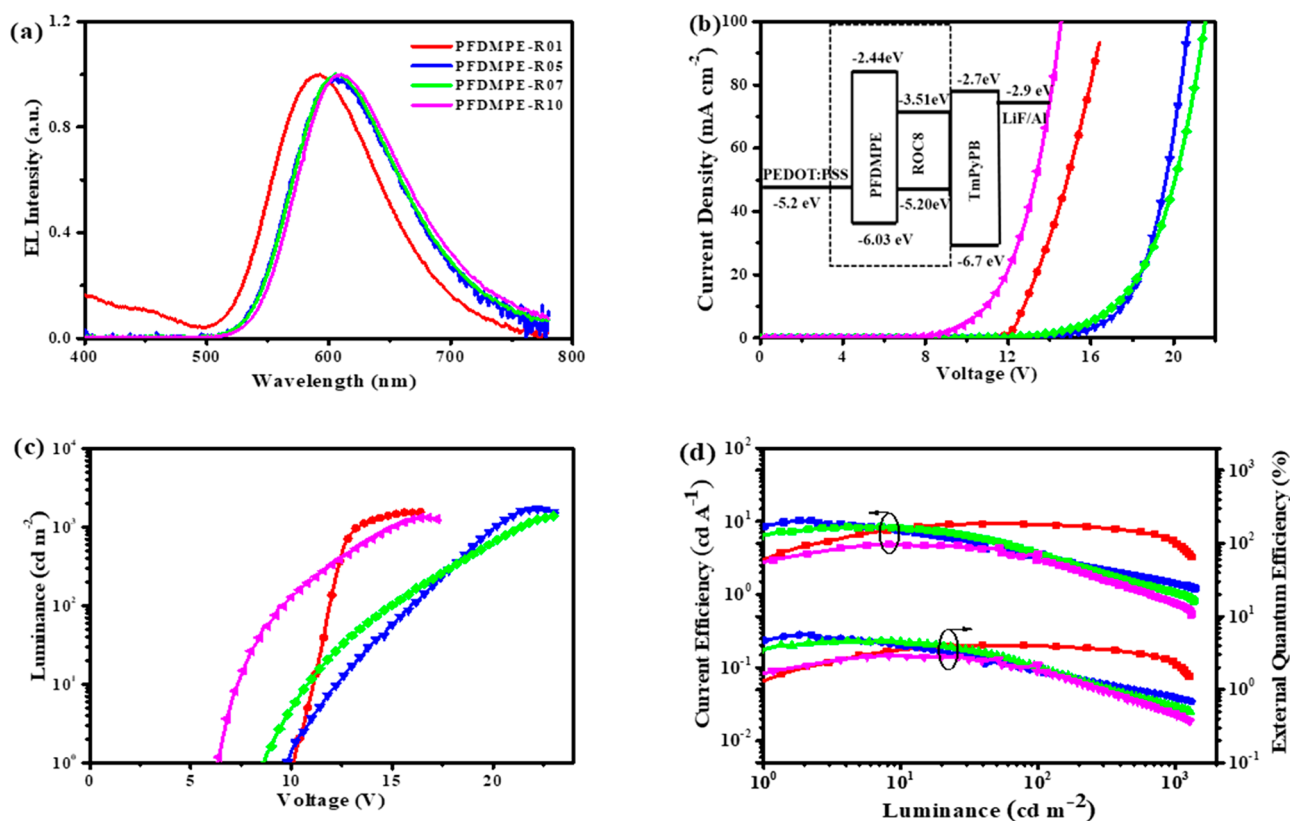


**Figure 7.** Device performance for red-emitting TADF polymers PFDMPPE-R01 to PFDMPPE-R010: (a) EL spectra at 12 V; (b) current density–voltage plots and energy level alignment inset; (c) luminance–voltage plots; and (d) current efficiency and EQE as a function of current density.

**Table 3.** Device Performance of Red-Emitting TADF Polymers PFDMPPE-R01 to PFDMPPE-R010<sup>a</sup>

polymers	$V_{\text{on}}$ (V)	$L_{\text{max}}$ (cd/m <sup>2</sup> )	$CE_{\text{max}}$ (cd/A)	$PE_{\text{max}}$ (lm/W)	EQE (%)	$\lambda_{\text{em}}$ (nm)	CIE (x, y)
PFDMPPE-R01	10.2	1546	9.3	2.5	4.07 (3.19)	591	(0.49, 0.42)
PFDMPPE-R05	9.8	1677	10.3	3.2	5.62 (1.02)	606	(0.57, 0.42)
PFDMPPE-R07	8.6	1365	8.3	2.7	4.64 (0.83)	607	(0.58, 0.42)
PFDMPPE-R10	6.4	1275	4.8	2.1	2.90 (0.72)	611	(0.59, 0.41)

<sup>a</sup> $V_{\text{on}}$ : turn-on voltage at 1 cd/m<sup>2</sup>;  $L_{\text{max}}$ : maximum luminance;  $CE_{\text{max}}$ : maximum current efficiency;  $PE_{\text{max}}$ : maximum power efficiency; EQE: maximum external quantum efficiency, and data at 500 cd/m<sup>2</sup> are given in parentheses.

## 4. EXPERIMENTAL SECTION

**4.1. Measurements and Characterization.** <sup>1</sup>H and <sup>13</sup>C NMR spectra were recorded with a Bruker Avance 400 NMR spectrometer. MALDI/TOF (matrix-assisted laser desorption ionization/time-of-flight) mass spectra were performed on an AXIMA CFR MS apparatus (COMPACT). Molecular weights of the polymers were determined by GPC in THF using polystyrene as the standard. Thermal gravimetric analysis (TGA) and differential scanning calorimetry (DSC) were performed under a flow of nitrogen with PerkinElmer-TGA 7 and PerkinElmer-DSC7 systems, respectively. UV–vis absorption and PL spectra were measured with a PerkinElmer Lambda 35 UV–vis spectrometer and a PerkinElmer LS 50B spectrofluorometer, respectively. The PLQYs of the TADF polymer films on quartz plates were measured using a quantum yield measurement system (C10027, Hamamatsu Photonics) excited at 375 nm. The CV was performed on a CHI660a electrochemical analyzer with Bu<sub>4</sub>NClO<sub>4</sub> (0.1 mol/L) as the electrolyte at a scan rate of 100 mV/s. A glass carbon electrode, a saturated calomel electrode, and a Pt wire were used as the working electrode, the reference electrode, and the counter electrode, respectively. The model compound ROC8 was tested in solutions (dichloromethane and THF for anodic and cathodic sweeping, respectively), and the TADF polymers were directly spin-coated on the working electrode for the measurement in acetonitrile. All the potentials were calibrated by

ferrocene/ferrocenium (Fc/Fc<sup>+</sup>). Fluorescence lifetime were carried out with Edinburgh fluorescence spectrometer (FLS980).

**4.2. Device Fabrication and Testing.** The indium tin oxide (ITO) (20 Ω/square) substrates were cleaned with acetone, detergent, and distilled water and then in an ultrasonic solvent bath. After baking in a heating chamber at 130 °C for 2 h, the ITO-glass substrates were treated with UV-ozone for 25 min. First, PEDOT:PSS (Batron-P4083, Bayer AG) was spin-coated on top of the ITO at a speed of 5000 rpm for 60 s and baked at 120 °C for 45 min. After being transferred into a nitrogen-filled glovebox, subsequently, solutions of the TADF polymers in toluene were spin-coated on PEDOT:PSS as the emissive layer at a speed of 1500 rpm for 60 s and annealed at 80 °C for 0.5 h. Finally, the other layers including TmPyPB (50 nm), LiF (1 nm), and Al (100 nm) were deposited in a vacuum chamber at a base pressure of less than 4 × 10<sup>-4</sup> Pa. The EL spectra and CIE coordinates were measured using a PR650 spectra colorimeter. The current–voltage and brightness–voltage curves of devices were measured using a Keithley 2400/2000 source meter and a calibrated silicon photodiode. All the measurements were performed at room temperature under ambient conditions.

**4.3. Synthesis.** All chemicals and reagents were used as received from commercial sources without further purification. Solvents for

chemical synthesis were purified according to the standard procedures.

**4-Bromo-*N*-(4-methoxyphenyl)diphenylamine (1).** 4-Bromodiphenylamine (40.00 g, 161.20 mmol), *p*-iodoanisole (49.05 g, 209.60 mmol), 1,10-phenanthroline monohydrate (2.90 g, 16.12 mmol), CuCl (1.61 g, 16.12 mmol), and KOH (90.16 g, 1610.00 mmol) were charged in a 1000 mL three-neck flask, and then 600 mL of dry toluene was added. The mixture was heated to 110 °C under argon and stirred for 36 h. After cooling to room temperature, the mixture was extracted with dichloromethane, washed with deionized water, dried by anhydrous sodium sulfate, and concentrated under vacuum. The crude product was purified by column chromatography on silica gel using petroleum ether/ethyl acetate (*v/v* = 25/1) as eluent to give **1** as a colorless oil (27.00 g, 60%). <sup>1</sup>H NMR (400 MHz, C<sub>6</sub>D<sub>6</sub>): δ 7.12 (m, 2H), 7.08–6.97 (m, 4H), 6.93–6.87 (m, 2H), 6.86–6.80 (m, 1H), 6.78–6.71 (m, 2H), 6.69–6.62 (m, 2H), 3.27 (s, 3H).

**4-Bromo-*N*-(4-hydroxyphenyl)diphenylamine (2).** Compound **1** (26.70 g, 75.42 mmol) was charged into a 500 mL three-neck flask, to which was added 300 mL of dry dichloromethane. Then BBr<sub>3</sub> (21.42 mL, 2.65 g/mL) was dropwisely added to the flask under argon at 0 °C. After the mixture was stirred for 5 h, the reaction was quenched by water. The mixture was washed with water, dried by anhydrous sodium sulfate, and then concentrated. Purification of the crude product by column chromatography on silica gel using petroleum ether/dichloromethane (*v/v* = 10/1) as eluent give **2** as a colorless oil (21.74 g, 85%). <sup>1</sup>H NMR (400 MHz, *d*<sub>6</sub>-DMSO): δ 9.43 (s, 1H), 7.35 (d, *J* = 8.8 Hz, 2H), 7.26 (t, *J* = 7.8 Hz, 2H), 7.03–6.88 (m, 5H), 6.83–6.73 (m, 4H).

**4-(4,4,5,5-Tetramethyl-1,3,2-dioxaborolan-2-yl)-*N*-(4-hydroxyphenyl)diphenylamine (3).** Compound **2** (17.37 g, 51.10 mmol), bis(pinacolato)diboron (19.46 g, 76.60 mmol), potassium acetate (15.00 g, 153.3 mmol), and Pd(dppf)Cl<sub>2</sub> (1.25 g, 1.53 mmol) were dissolved in 150 mL of dry DMF under argon. The mixture was stirred at 85 °C for 24 h. After cooling to room temperature, the mixture was extracted with dichloromethane three times. The organic phase was combined and washed with water, dried by anhydrous sodium sulfate, and then concentrated under vacuum. The crude product was applied to column chromatography on silica gel with petroleum ether/ethyl acetate (*v/v* = 5/1) as eluent to give **3** as a white powder (11.47 g, 58%). <sup>1</sup>H NMR (400 MHz, *d*<sub>6</sub>-DMSO): δ 9.49 (s, 1H), 7.48 (d, *J* = 7.9 Hz, 2H), 7.29 (t, *J* = 7.6 Hz, 2H), 7.03 (d, *J* = 7.8 Hz, 3H), 6.94 (d, *J* = 8.4 Hz, 2H), 6.78 (dd, *J* = 7.8, 3.6 Hz, 4H), 1.26 (s, 12H).

**2-(*N*-(4-Hydroxyphenyl)diphenylamino)-4'-anthraquinone (4).** Compound **3** (7.60 g, 19.64 mmol), 2-bromoanthracene-9,10-dione (5.13 g, 17.85 mmol), tetrakis(triphenylphosphine)palladium (0.41 g, 0.36 mmol), and Aliquat 336 (0.1 mL) were added to a mixture of toluene (200 mL) and aqueous K<sub>2</sub>CO<sub>3</sub> (17.85 mL, 2 M) under argon. The mixture was heated to 100 °C and stirred for 24 h. After cooling to room temperature, the mixture was extracted with dichloromethane and then washed with water. The organic phase was dried by anhydrous sodium sulfate and then concentrated under vacuum. The residue was purified by column chromatography on silica gel with petroleum ether/ethyl acetate (*v/v* = 5/1) as eluent to give **4** as a red powder (2.27 g, 75%). <sup>1</sup>H NMR (400 MHz, *d*<sub>6</sub>-DMSO): δ 9.53 (s, 1H), 8.36 (s, 1H), 8.23 (d, *J* = 8.1 Hz, 3H), 8.17 (d, *J* = 8.0 Hz, 1H), 8.00–7.88 (m, 2H), 7.73 (d, *J* = 8.4 Hz, 2H), 7.33 (t, *J* = 7.7 Hz, 2H), 7.13–7.05 (m, 3H), 7.05–6.99 (m, 2H), 6.97 (d, *J* = 8.5 Hz, 2H), 6.81 (d, *J* = 8.5 Hz, 2H).

**2-(*N*-(4-(8-Bromooctyl)oxy)phenyl)diphenylamino)-4'-anthraquinone (5).** A mixture of **4** (7.85 g, 16.79 mmol), 1, 8-dibromooctane (22.83 g, 83.95 mmol), K<sub>2</sub>CO<sub>3</sub> (11.56 g, 83.95 mmol), and tetrabutylammonium bromide (0.27 g, 0.84 mmol) were dissolved in 200 mL of THF under argon. The mixture was heated to reflux and stirred for 12 h. After cooling to room temperature, the mixture was extracted with dichloromethane three times. The combined organic phase was dried by anhydrous sodium sulfate and then concentrated under vacuum. Purification of the crude product by column chromatography on silica gel with petroleum

ether/ethyl acetate (*v/v* = 20/1) as eluent to give **5** as a red powder (8.63 g, 78%). <sup>1</sup>H NMR (400 MHz, CDCl<sub>3</sub>): δ 8.51 (d, *J* = 1.5 Hz, 1H), 8.34 (dd, *J* = 8.5, 3.2 Hz, 3H), 7.98 (dd, *J* = 8.2, 1.7 Hz, 1H), 7.86–7.77 (m, 2H), 7.60 (d, *J* = 8.6 Hz, 2H), 7.29 (d, *J* = 7.9 Hz, 2H), 7.19–7.09 (m, 7H), 6.88 (d, *J* = 8.9 Hz, 2H), 3.96 (t, *J* = 6.4 Hz, 2H), 3.42 (t, *J* = 6.8 Hz, 2H), 1.96–1.72 (m, 4H), 1.61–1.25 (m, 8H).

**2-(*N*-(4-(8-(2,7-Dibromo-9-octylfluoren-9-yl)octyl)oxy)phenyl)diphenylamino)-4'-anthraquinone (6).** A mixture of **5** (5.20 g, 7.90 mmol), 2,7-dibromo-9-octylfluorene (3.96 g, 9.08 mmol), and KOH (4.42 g, 79.00 mmol) were dissolved in 150 mL of DMF under argon. The mixture was heated to 70 °C and stirred for 12 h. After cooling to room temperature, the mixture was extracted with dichloromethane and washed with water. After the organic phase was dried by anhydrous sodium sulfate and concentrated under vacuum, the crude product was purified by column chromatography on silica gel with petroleum ether/ethyl acetate (*v/v* = 30/1) as eluent. After recrystallized from ethanol, the monomer **6** was obtained as a red acicular crystal (5.30 g, 65%). <sup>1</sup>H NMR (400 MHz, *d*<sub>6</sub>-DMSO): δ 8.37 (d, *J* = 1.6 Hz, 1H), 8.24 (m, 3H), 8.18 (m, 1H), 7.95 (m, 2H), 7.85–7.71 (m, 4H), 7.68 (d, *J* = 1.6 Hz, 2H), 7.58–7.49 (m, 2H), 7.37–7.30 (m, 2H), 7.08 (t, *J* = 8.0 Hz, 5H), 6.96 (m, 4H), 3.90 (t, *J* = 6.2 Hz, 2H), 2.07–1.94 (m, 4H), 1.61 (m, 2H), 1.14 (m, 18H), 0.78 (t, *J* = 7.1 Hz, 3H), 0.44 (m, 4H). <sup>13</sup>C NMR (126 MHz, CDCl<sub>3</sub>): δ 183.43, 182.84, 156.34, 152.68, 152.07, 149.15, 147.39, 146.39, 139.77, 139.08, 138.43, 134.12, 133.92, 133.77, 133.67, 132.45, 131.40, 131.37, 130.90, 130.37, 130.17, 129.41, 129.30, 128.08, 127.90, 127.79, 127.36, 127.24, 127.18, 126.16, 124.58, 124.10, 123.00, 121.48, 121.32, 121.15, 115.48, 68.33, 57.15, 55.71, 40.17, 40.12, 37.98, 32.57, 31.81, 31.61, 29.94, 29.76, 29.24, 29.19, 29.17, 29.14, 29.10, 28.77, 25.95, 23.60, 22.50, 14.12. MALDI-TOF MS: *m/z* 1013.3.

**4,4'-Oxybis(1-bromo-2-methylbenzene) (7).** 4-Bromo-3-methylphenol (20.00 g, 107.00 mmol), 1-bromo-4-iodo-2-methylbenzene (41.28 g, 139.00 mmol), CuI (0.20 g, 1.07 mmol), 2,2,6,6-tetramethylheptane-3,5-dione (1.97 g, 10.70 mmol), and Cs<sub>2</sub>CO<sub>3</sub> (69.76 g, 214 mmol) were added in 100 mL of DMF under argon. The mixture was heated to 110 °C and stirred for 15 h. After the reaction was finished, the mixture was extracted with dichloromethane. The combined organic phase was washed with water and then dried by anhydrous sodium sulfate. After removal of the solvent under vacuum, the crude product was purified by column chromatography on silica gel with *n*-hexane as eluent to give **7** as a white solid (26.00 g, 70%). <sup>1</sup>H NMR (400 MHz, CDCl<sub>3</sub>): δ 7.45 (d, *J* = 6.9 Hz, 2H), 6.87 (d, *J* = 2.8 Hz, 2H), 6.69 (dd, *J* = 8.6, 2.9 Hz, 2H), 2.36 (s, 6H).

**2,2'-(Oxybis(2-methyl-4,1-phenylene))bis(4,4,5,5-tetramethyl-1,3,2-dioxaborolane) (8).** To a 250 mL three-neck flask was added **7** (15.00 g, 42.13 mmol), bis(pinacolato)diboron (27.82 g, 109.54 mmol), Pd(dppf)Cl<sub>2</sub> (4.13 g, 5.06 mmol), KOAc (28.90 g, 294.91 mmol), and 120 mL of dry DMF under argon. The mixture was heated to 110 °C and stirred for 24 h. After cooling to room temperature, the mixture was extracted with dichloromethane three times. The combined organic phase was washed with water, dried by anhydrous sodium sulfate, and concentrated under vacuum. The crude product was applied to column chromatography on silica gel with petroleum ether/ethyl acetate (*v/v* = 30/1) as eluent. After recrystallized from a mixture of methylene chloride and ethanol, the monomer **8** was obtained as a white needle crystal (11.34 g, 60%). <sup>1</sup>H NMR (400 MHz, CDCl<sub>3</sub>): δ 7.73 (dd, *J* = 7.3, 1.5 Hz, 2H), 6.80 (s, 3H), 6.78 (s, 1H), 2.50 (s, 6H), 1.33 (s, 24H). <sup>13</sup>C NMR (126 MHz, CDCl<sub>3</sub>): δ 159.13, 147.47, 137.89, 120.17, 115.03, 83.35, 24.94, 21.89. MALDI-TOF MS: *m/z* 450.3.

**General Synthesis of Red-Emitting TADF Polymers with PFDMPPE-R01 as an Example.** 2,7-Dibromo-9,9-dioctylfluorene (0.1357 g, 0.2475 mmol), monomer **6** (0.0025 g, 0.0025 mmol), monomer **8** (0.1125 g, 0.25 mmol), Pd<sub>2</sub>(dba)<sub>3</sub> (1.0 mg, 0.001 mmol), 2-dicyclohexylphosphino-2',6'-dimethoxybiphenyl (S-Phos) (3.1 mg, 0.0075 mmol), and Aliquat 336 (0.1 mL) were added to a mixture of toluene (5 mL) and aqueous K<sub>2</sub>CO<sub>3</sub> (2.5 mL, 2 M) under argon. The

mixture was heated to 95 °C and stirred for 5 h. Subsequently, benzenboronic acid (30 mg) in 5 mL of toluene was added, and the mixture was refluxed for 5 h. Then 0.5 mL of bromobenzene was added, and the mixture was kept refluxed for another 5 h. Finally, sodium diethyldithiocarbamate trihydrate (1.0 g) dissolved in deionized water (15 mL) was added into the mixture. The solution was kept at 80 °C with vigorous stirring under argon for 24 h. After cooling to room temperature, the mixture was extracted by dichloromethane, which was washed five times with deionized water and dried by anhydrous sodium sulfate. After removal of the solvent, the resulting polymers were received by precipitation in methanol. The final purification was performed by Soxhlet extraction with acetone for about 24 h and then precipitated in methanol to give the desired polymer PFDMPPE-R01 (96.0 mg, 65%). <sup>1</sup>H NMR (400 MHz, CDCl<sub>3</sub>): δ 8.51 (s, 0.0109H), 8.34 (d, J = 6.4 Hz, 0.0329H), 7.98 (d, J = 9.3 Hz, 0.0363H), 7.78 (d, J = 8.1 Hz, 2H), 7.59 (d, J = 8.6 Hz, 0.0661H), 7.52 (s, 0.0681H), 7.33 (d, J = 6.2 Hz, 6H), 7.17–7.10 (m, 0.1512H), 7.05 (s, 2H), 7.01 (d, J = 7.9 Hz, 2H), 6.85 (d, J = 8.5 Hz, 0.0745H), 3.90 (s, 0.0288H), 2.33 (s, 6H), 2.01 (s, 4H), 1.31–0.99 (m, 20H), 0.82 (t, J = 7.0 Hz, 6H), 0.76 (s, 4H). <sup>13</sup>C NMR (101 MHz, CDCl<sub>3</sub>): δ 156.44, 150.85, 140.16, 139.65, 137.73, 137.40, 131.19, 128.14, 124.10, 120.64, 119.40, 116.26, 55.23, 40.51, 31.87, 30.11, 29.34, 29.28, 23.98, 22.70, 20.92, 14.16.

**PFDMPPE-R05 (106.8 mg, 70%).** 2,7-Dibromo-9,9-dioctylfluorene (0.1303 g, 0.2375 mmol), monomer **6** (0.0127 g, 0.0125 mmol), and monomer **8** (0.1125 g, 0.25 mmol) were used. <sup>1</sup>H NMR (400 MHz, CDCl<sub>3</sub>): δ 8.51 (s, 0.0490H), 8.34 (m, 0.1448H), 7.97 (d, J = 7.5 Hz, 0.0810H), 7.78 (d, J = 8.0 Hz, 2H), 7.59 (d, J = 7.6 Hz, 0.1430H), 7.52 (s, 0.0784H), 7.33 (d, J = 7.0 Hz, 6H), 7.17–7.10 (m, 0.3770H), 7.05 (s, 2H), 7.01 (d, J = 8.1 Hz, 2H), 6.85 (d, J = 8.4 Hz, 0.2015H), 3.90 (s, 0.1039H), 2.33 (s, 6H), 2.01 (s, 4H), 1.31–0.99 (m, 20H), 0.82 (t, J = 7.0 Hz, 6H), 0.76 (s, 4H). <sup>13</sup>C NMR (101 MHz, CDCl<sub>3</sub>): δ 156.43, 150.85, 140.16, 139.65, 137.73, 137.40, 131.19, 128.14, 124.09, 120.64, 119.40, 116.26, 55.22, 40.51, 31.86, 30.10, 29.34, 29.28, 23.98, 22.70, 20.92, 14.17.

**PFDMPPE-R07 (100.4 mg, 65%).** 2,7-Dibromo-9,9-dioctylfluorene (0.1275 g, 0.2325 mmol), monomer **6** (0.0177 g, 0.0175 mmol), and monomer **8** (0.1125 g, 0.25 mmol) were used. <sup>1</sup>H NMR (400 MHz, CDCl<sub>3</sub>): δ 8.51 (s, 0.0675H), 8.34 (d, J = 6.4 Hz, 0.1876H), 7.97 (d, J = 8.2 Hz, 0.1120H), 7.78 (d, J = 8.0 Hz, 2H), 7.59 (d, J = 8.5 Hz, 0.1869H), 7.52 (s, 0.0879H), 7.33 (d, J = 6.0 Hz, 6H), 7.17–7.09 (m, 0.6322H), 7.05 (s, 2H), 7.01 (d, J = 7.9 Hz, 2H), 6.85 (d, J = 8.8 Hz, 0.2346H), 3.90 (s, 0.1361H), 2.33 (s, 6H), 2.01 (s, 4H), 1.31–0.99 (m, 20H), 0.82 (t, J = 7.0 Hz, 6H), 0.76 (s, 4H). <sup>13</sup>C NMR (101 MHz, CDCl<sub>3</sub>): δ 156.44, 150.85, 140.17, 139.65, 137.73, 137.40, 131.19, 128.14, 124.10, 120.64, 119.40, 116.26, 55.23, 40.51, 31.86, 30.10, 29.33, 29.27, 23.97, 22.69, 20.91, 14.16.

**PFDMPPE-R10 (110.7 mg, 70%).** 2,7-Dibromo-9,9-dioctylfluorene (0.1234 g, 0.225 mmol), monomer **6** (0.0253 g, 0.025 mmol), and monomer **8** (0.1125 g, 0.25 mmol) were used. <sup>1</sup>H NMR (400 MHz, CDCl<sub>3</sub>): δ 8.51 (s, 0.1030H), 8.33 (s, 0.2815H), 7.98 (d, J = 7.7 Hz, 0.1870H), 7.78 (d, J = 6.7 Hz, 2H), 7.59 (d, J = 7.7 Hz, 0.2692H), 7.52 (s, 0.1269H), 7.34 (s, 6H), 7.17–7.10 (m, 0.7105H), 7.05 (s, 2H), 7.01 (d, J = 6.9 Hz, 2H), 6.85 (d, J = 8.1 Hz, 0.2520H), 3.90 (s, 0.1800H), 2.33 (s, 6H), 2.01 (s, 4H), 1.31–0.99 (m, 20H), 0.82 (t, J = 7.0 Hz, 6H), 0.76 (s, 4H). <sup>13</sup>C NMR (101 MHz, CDCl<sub>3</sub>): δ 183.48, 182.96, 156.44, 150.86, 140.17, 139.66, 137.74, 137.40, 134.17, 134.00, 133.89, 133.74, 131.44, 131.19, 129.42, 128.14, 127.99, 127.86, 127.32, 127.26, 124.65, 124.10, 123.03, 121.67, 120.65, 119.40, 116.26, 115.56, 68.27, 55.23, 40.51, 31.86, 30.10, 29.34, 29.27, 26.06, 23.98, 22.69, 20.91, 14.16.

**PFDMPPE (102.6 mg, 70%).** 2,7-Dibromo-9,9-dioctylfluorene (0.1371 g, 0.25 mmol) and monomer **8** (0.1125 g, 0.25 mmol) were used. <sup>1</sup>H NMR (400 MHz, CDCl<sub>3</sub>): δ 7.78 (d, J = 8.0 Hz, 2H), 7.33 (d, J = 6.1 Hz, 6H), 7.05 (s, 2H), 7.00 (d, J = 8.2 Hz, 2H), 2.33 (s, 6H), 2.01 (s, 4H), 1.31–0.99 (m, 20H), 0.82 (t, J = 7.0 Hz, 6H), 0.76 (s, 4H). <sup>13</sup>C NMR (101 MHz, CDCl<sub>3</sub>): δ 156.44, 150.85, 140.16, 139.65, 137.73, 137.40, 131.19, 128.14, 124.10, 120.64, 119.40, 116.26, 55.23, 40.51, 31.86, 30.11, 29.34, 29.28, 23.98, 22.70, 20.91, 14.16.

## ■ ASSOCIATED CONTENT

### ● Supporting Information

The Supporting Information is available free of charge on the ACS Publications website at DOI: 10.1021/acs.macromol.8b02050.

Figures S1–S18 (DOCX)

## ■ AUTHOR INFORMATION

### Corresponding Authors

\*E-mail wangshumeng@ciac.ac.cn.

\*E-mail junqiaod@ciac.ac.cn.

### ORCID

Junqiao Ding: 0000-0001-7719-6599

Lixiang Wang: 0000-0002-4676-1927

### Notes

The authors declare no competing financial interest.

## ■ ACKNOWLEDGMENTS

The authors acknowledge the financial support from the National Key Research and Development Program (2016YFB0401301), the 973 Project (2015CB655001), and the National Natural Science Foundation of China (Nos. 51873205 and 51573183).

## ■ REFERENCES

- (1) Burroughes, J. H.; Bradley, D. D. C.; Brown, A. R.; Marks, R. N.; Mackay, K.; Friend, R. H.; Burns, P. L.; Holmes, A. B. Light-Emitting Diodes Based on Conjugated Polymers. *Nature* **1990**, *347*, 539.
- (2) Grimsdale, A. C.; Chan, K. L.; Martin, R. E.; Jokisz, P. G.; Holmes, A. B. Synthesis of Light-Emitting Conjugated Polymers for Applications in Electroluminescent Devices. *Chem. Rev.* **2009**, *109*, 897.
- (3) Xu, F.; Kim, H. U.; Kim, J.-H.; Jung, B. J.; Grimsdale, A. C.; Hwang, D.-H. Progress and Perspective of Iridium-Containing Phosphorescent Polymers for Light-Emitting Diodes. *Prog. Polym. Sci.* **2015**, *47*, 92.
- (4) Shao, S.; Ding, J.; Wang, L. New Applications of Poly(arylene ether)s in Organic Light-Emitting Diodes. *Chin. Chem. Lett.* **2016**, *27*, 1201.
- (5) Shao, S.; Ding, J.; Wang, L. Research Progress on Electroluminescent Polymers. *Acta Polym. Sin.* **2018**, *2*, 198.
- (6) Zou, Y.; Gong, S.; Xie, G.; Yang, C. Design Strategy for Solution-Processable Thermally Activated Delayed Fluorescence Emitters and Their Applications in Organic Light-Emitting Diodes. *Adv. Opt. Mater.* **2018**, 1800568.
- (7) Liu, Y.; Li, C.; Ren, Z.; Yan, S.; Bryce, M. R. All-Organic Thermally Activated Delayed Fluorescence Materials for Organic Light-Emitting Diodes. *Nature Rev. Mater.* **2018**, *3*, 18020.
- (8) Xu, X.; Li, X.; Wang, S.; Ding, J.; Wang, L. Deep-Blue Emitting Poly[spiro(dibenzoazasilene-10',9-silafluorene)] for Power-Efficient PLEDs. *J. Mater. Chem. C* **2018**, *6*, 9599.
- (9) Bai, K.; Wang, S.; Zhao, L.; Ding, J.; Wang, L. Efficient Blue, Green, and Red Electroluminescence from Carbazole-Functionalized Poly(spirobifluorene)s. *Macromolecules* **2017**, *50*, 6945.
- (10) Shao, S.; Ding, J.; Wang, L.; Jing, X.; Wang, F. Highly Efficient Blue Electrophosphorescent Polymers with Fluorinated Poly(arylene ether phosphine oxide) as Backbone. *J. Am. Chem. Soc.* **2012**, *134*, 15189.
- (11) Nikolaenko, A. E.; Cass, M.; Bourcet, F.; Mohamad, D.; Roberts, M. Thermally Activated Delayed Fluorescence in Polymers: A New Route toward Highly Efficient Solution Processable OLEDs. *Adv. Mater.* **2015**, *27*, 7236.
- (12) Uoyama, H.; Goushi, K.; Shizu, K.; Nomura, H.; Adachi, C. Highly Efficient Organic Light-Emitting Diodes from Delayed Fluorescence. *Nature* **2012**, *492*, 234.

- (13) Lee, S. Y.; Yasuda, T.; Komiyama, H.; Lee, J.; Adachi, C. Thermally Activated Delayed Fluorescence Polymers for Efficient Solution-Processed Organic Light-Emitting Diodes. *Adv. Mater.* **2016**, *28*, 4019.
- (14) Wang, Y.; Zhu, Y.; Xie, G.; Zhan, H.; Yang, C.; Cheng, Y. Bright White Electroluminescence from a Single Polymer Containing a Thermally Activated Delayed Fluorescence Unit and a Solution-Processed Orange OLED Approaching 20% External Quantum Efficiency. *J. Mater. Chem. C* **2017**, *5*, 10715.
- (15) Ren, Z.; Nobuyasu, R. S.; Dias, F. B.; Monkman, A. P.; Yan, S.; Bryce, M. R. Pendant Homopolymer and Copolymers as Solution-Processable Thermally Activated Delayed Fluorescence Materials for Organic Light-Emitting Diodes. *Macromolecules* **2016**, *49*, 5452.
- (16) Xie, G.; Luo, J.; Huang, M.; Chen, T.; Wu, K.; Gong, S.; Yang, C. Inheriting the Characteristics of TADF Small Molecule by Side-Chain Engineering Strategy to Enable Bluish-Green Polymers with High PLQYs up to 74% and External Quantum Efficiency over 16% in Light-Emitting Diodes. *Adv. Mater.* **2017**, *29*, 1604223.
- (17) Shao, S.; Hu, J.; Wang, X.; Wang, L.; Jing, X.; Wang, F. Blue Thermally Activated Delayed Fluorescence Polymers with Non-conjugated Backbone and Through-Space Charge Transfer Effect. *J. Am. Chem. Soc.* **2017**, *139*, 17739.
- (18) Li, C.; Nobuyasu, R. S.; Wang, Y.; Dias, F. B.; Ren, Z.; Bryce, M. R.; Yan, S. Solution-Processable Thermally Activated Delayed Fluorescence White OLEDs Based on Dual-Emission Polymers with Tunable Emission Colors and Aggregation-Enhanced Emission Properties. *Adv. Opt. Mater.* **2017**, *5*, 1700435.
- (19) Li, C.; Wang, Y.; Sun, D.; Li, H.; Sun, X.; Ma, D.; Ren, Z.; Yan, S. Thermally Activated Delayed Fluorescence Pendant Copolymers with Electron- and Hole-Transporting Spacers. *ACS Appl. Mater. Interfaces* **2018**, *10*, 5731.
- (20) Kim, J. H.; Yun, J. H.; Lee, J. Y. Recent Progress of Highly Efficient Red and Near-Infrared Thermally Activated Delayed Fluorescent Emitters. *Adv. Opt. Mater.* **2018**, *6*, 1800255.
- (21) Zhang, Q.; Kuwabara, H.; Potscavage, W. J.; Huang, S.; Hatae, Y.; Shibata, T.; Adachi, C. Anthraquinone-Based Intramolecular-Charge-Transfer Compounds: Computational Molecular Design, Thermally Activated Delayed Fluorescence, and Highly-Efficient Red Electroluminescence. *J. Am. Chem. Soc.* **2014**, *136*, 18070.
- (22) Sagara, Y.; Shizu, K.; Tanaka, H.; Miyazaki, H.; Goushi, K.; Kaji, H.; Adachi, C. Highly Efficient Thermally Activated Delayed Fluorescence Emitters with a Small Singlet–Triplet Energy Gap and Large Oscillator Strength. *Chem. Lett.* **2015**, *44*, 360.
- (23) Sudhakar, M.; Djurovich, P. I.; Hogen-Esch, T. E.; Thompson, M. E. Phosphorescence Quenching by Conjugated Polymers. *J. Am. Chem. Soc.* **2003**, *125*, 7796.
- (24) Lee, S. Y.; Yasuda, T.; Nomura, H.; Adachi, C. High-Efficiency Organic Light-Emitting Diodes Utilizing Thermally Activated Delayed Fluorescence from Triazine-Based Donor–Acceptor Hybrid Molecules. *Appl. Phys. Lett.* **2012**, *101*, 093306.
- (25) Kim, B. S.; Lee, J. Y. Engineering of Mixed Host for High External Quantum Efficiency above 25% in Green Thermally Activated Delayed Fluorescence Device. *Adv. Funct. Mater.* **2014**, *24*, 3970.
- (26) Andrews, D. L.; Juzeliūnas, G. Intermolecular Energy Transfer: Retardation Effects. *J. Chem. Phys.* **1992**, *96*, 6606.
- (27) Caspar, J. V.; Kober, E. M.; Sullivan, B. P.; Meyer, T. J. Application of the Energy Gap Law to the Decay of Charge-Transfer Excited States. *J. Am. Chem. Soc.* **1982**, *104*, 630.
- (28) Kim, G. H.; Lampande, R.; Im, J. B.; Lee, J. M.; Lee, J. Y.; Kwon, J. H. Controlling the Exciton Lifetime of Blue Thermally Activated Delayed Fluorescence Emitters Using a Heteroatom-Containing Pyridoindole Donor Moiety. *Mater. Horiz.* **2017**, *4*, 619.
- (29) Xiang, Y.; Zhu, Z.-L.; Xie, D.; Gong, S.; Wu, K.; Xie, G.; Lee, C.-S.; Yang, C. Revealing the New Potential of an Indandione Unit for Constructing Efficient Yellow Thermally Activated Delayed Fluorescence Emitters with Short Emissive Lifetimes. *J. Mater. Chem. C* **2018**, *6*, 7111.
- (30) Endo, A.; Sato, K.; Yoshimura, K.; Kai, T.; Kawada, A.; Miyazaki, H.; Adachi, C. Efficient Up-Conversion of Triplet Excitons into a Singlet State and its Application for Organic Light Emitting Diodes. *Appl. Phys. Lett.* **2011**, *98*, 083302.
- (31) Li, J.; Nakagawa, T.; MacDonald, J.; Zhang, Q.; Nomura, H.; Miyazaki, H.; Adachi, C. Highly Efficient Organic Light-Emitting Diode Based on a Hidden Thermally Activated Delayed Fluorescence Channel in a Heptazine Derivative. *Adv. Mater.* **2013**, *25*, 3319.
- (32) Su, S.-J.; Chiba, T.; Takeda, T.; Kido, J. Pyridine-Containing Triphenylbenzene Derivatives with High Electron Mobility for Highly Efficient Phosphorescent OLEDs. *Adv. Mater.* **2008**, *20*, 2125.
- (33) Chen, X.; Liao, J.-L.; Liang, Y.; Ahmed, M. O.; Tseng, H.-E.; Chen, S.-A. High-Efficiency Red-Light Emission from Polyfluorenes Grafted with Cyclometalated Iridium Complexes and Charge Transport Moiety. *J. Am. Chem. Soc.* **2003**, *125*, 636.
- (34) Jiang, J.; Jiang, C.; Yang, W.; Zhen, H.; Huang, F.; Cao, Y. High-Efficiency Electrophosphorescent Fluorene-alt-Carbazole Copolymers N-Grafted with Cyclometalated Ir Complexes. *Macromolecules* **2005**, *38*, 4072.
- (35) Ma, Z.; Ding, J.; Zhang, B.; Mei, C.; Cheng, Y.; Xie, Z.; Wang, L.; Jing, X.; Wang, F. Red-Emitting Polyfluorenes Grafted with Quinoline-Based Iridium Complex: “Simple Polymeric Chain, Unexpected High Efficiency. *Adv. Funct. Mater.* **2010**, *20*, 138.